



Chemical modification of biochar's functional groups enhances phosphate and arsenite adsorption

Md. Rayhan Ahmed¹, Shamim Mia^{2,3*}, Md. Abdus Sattar¹, M. M. Masud⁴, S. M. Mahabubul Alam², Sohela Akter⁴, Md. Sharif Mia², Sanjida Aktar⁵

¹ Department of Emergency Management, Faculty of Environmental Science and Disaster Management, Patuakhali Science and Technology University, Dumki-8602, Bangladesh

² Department of Agronomy, Patuakhali Science and Technology University, Dumki-8602, Bangladesh

³ School Life and Environmental Sciences, The University of Sydney, Australia

⁴ Soil Science Division, Bangladesh Agriculture Research Institute, Gazipur- 1701, Bangladesh

⁵ Department of Environmental Science, Faculty of Environmental Science and Disaster Management, Patuakhali Science and Technology University, Dumki-8602, Bangladesh

ARTICLE INFO

Keywords:

Anionic species
Functionality
Mechanisms
Pyrogenic carbon
Sorption

Article history

Submitted: 2024-08-24

Revised: 2025-04-16

Accepted: 2025-05-30

Available online: 2025-06-29

Published regularly:

June 2025

* Corresponding Author

Email address:

smia_agr@pstu.ac.bd

ABSTRACT

Anionic arsenic (As) species and phosphate often show similar behavior in soils. Bioavailability of these anionic species has a significant implication for crop production and soil health. Biochar (BC) is considered an effective amendment for managing these anionic species. This study aims to evaluate how surface-modified biochars influence phosphate and arsenite adsorption. Biochars with a range of functionalities were produced using mineral doping, and chemical oxidation with hydrogen peroxide. These biochars were then characterized using different chemical techniques, including FTIR. Next, a phosphorus adsorption study was conducted with fresh, mineral-doped and chemically oxidized biochars. A desorption study was also conducted to understand the strength of sorption. Moreover, an adsorption study was carried out using three different biochars fresh, oxidized, and doped in interaction with As. Our results showed that chemical oxidation increased oxygen-containing functional groups while mineral impregnation decreased their presence, resulting in a reduction in cation exchange capacity. As a result, phosphate adsorption was significantly higher with mineral- doped biochar (2.5 mg g⁻¹ biochar) than in fresh biochar (2.2 mg g⁻¹ biochar) treatment. The strength of binding was higher for positively charged biochars. Similar to phosphate, the As adsorption was also higher in the doped biochar (~0.50 mg g⁻¹ biochar) than oxidized biochar (0.20 mg g⁻¹biochar). Surprisingly, the As adsorption was higher in the oxidized BC than fresh BC possibly due to its co-adsorption with cations. Altogether, our results suggest that biochar with positive surfaces could strongly bind negatively charged ions from aqueous solutions and soils.

How to Cite: Ahmed, M.R., Mia, S., Sattar, M.A., Masud, M.M., Alam, S.M.M., Akter, S., Mia, M.S., Aktar, S. (2025). Chemical modification of biochar's functional groups enhances phosphate and arsenite adsorption. Sains Tanah Journal of Soil Science and Agroclimatology, 22(1), 203-219. <https://doi.org/10.20961/stjssa.v22i1.92550>

1. INTRODUCTION

Anionic species in soils, particularly phosphate and arsenate, often show similar behavior, although their roles are very different in plant performance (Strawn, 2018). Phosphorus is an essential plant nutrient, whereas arsenic (As) is a contaminant that negatively affects plant performance. Understanding their behavior, such as adsorption and desorption, can have significant implications for managing soil health and crop production.

Phosphorus bioavailability is a major constraint in many acid soils rich in Fe/Al oxides or hydroxides (Yan et al., 2020). The reason for the low bioavailability is the fixation of phosphate with soil minerals. In contrast, phosphate applications at higher rates, such as with animal manure, can cause environmental problems through increasing phosphate loading in water bodies (Yan et al., 2020). This particularly occurs when soil-positive reactive surfaces are low. Therefore, understanding phosphate dynamics in soil is

crucial, highlighting the need to enhance soil reactive surfaces for its better management.

Arsenic pollution is a serious problem in many countries including Bangladesh and around the world. Its concern is high due to its elevated toxicity and widespread environmental occurrence. Although the parent rock is the most abundant source of As in soils, anthropogenic activities have contributed significantly to the increase in its concentration in many soils (Ungureanu et al., 2015). The As present in soil can be taken up by plants and eventually enter into the human food chain, leading to potential exposure (Arslan et al., 2017). As a result, it presents a significant risk to human health and well-being (Ghezzi et al., 2023). Therefore, the development and adoption of effective remediation methods remain central in heavy metal research.

The bioavailability, transport, and uptake of anionic species such as phosphate and arsenite in the soils are largely controlled by soil-reactive surfaces (Caporale & Violante, 2016). The use of organic amendments can alter soil reactive surfaces, thereby influencing the speciation and retention of elements within the soil. Biochar, a pyrogenic carbon-rich material derived from pyrolysis, is valued for its roles in carbon storage capacity, soil fertility enhancement, and pollution control (Beesley et al., 2013; Mia et al., 2015; Namgay et al., 2010). Pyrogenic carbon including biochar, soot, black carbon and charcoal carries aromatic carbon and is usually created from incomplete combustion of biomass (Abney & Berhe, 2018; Singh et al., 2023). During incomplete burning, up to 25% of the carbon can convert into pyrogenic carbon (Cotrufo et al., 2016). Historically char added soil such as in Terra Preta soils is more productive due to its role in increasing soil pH, water retention capacity, and improving nutrient bioavailability (Reisser et al., 2016).

Biochar carries a large reactive surface with a large surface area and charge, enabling it to effectively adsorb anionic species (Mia et al., 2017b; Singh et al., 2023). The surface charge is associated with its functional groups that carry variable surface charges (Mia et al., 2017a, 2017b). Depending on production conditions and modifications, the functionality, i.e., the surface charge can be positive or neutral to negative (Mia et al., 2017a, 2017b). For instance, biochar carries a positive surface charge at pH ~7.0 when it is doped with Iron (Fe), Aluminum (Al), and Magnesium (Mg) minerals while it carries a negative charge when modified with chemical oxidizers such as hydrogen peroxide, and nitric acid (Mia et al., 2017a). Moreover, the properties of biochar change with time in the soil, a process known as aging (Mia et al., 2017a, 2017b). Especially, the net positive charge in the biochar surfaces changes to a net negative charge with the introduction of carboxylic and phenolic groups during aging (Mia et al., 2017a, 2017b). The specific surface area can also be changed with biochar aging or modifications. Therefore, understanding the extent in change of biochar properties through different modification (e.g., chemical, physical, or biological) treatments is crucial for their potential application in remediating arsenic (As)-contaminated soils (Liang et al., 2021). Engineered biochar with impregnation of iron (Fe) shows improved As fixation through surface complexation, redox chemical reactions, and co-precipitation mechanisms

(Wang et al., 2020). Biochar impregnation with Fe not only increases biochar's capability to adsorb arsenic but also reduces its bioavailability to plants by increasing its transformation into less mobile forms (Yin et al., 2017). Moreover, application of modified biochar into As-rich soils can boost soil fertility by enhancing nutrient retention (Zhang et al., 2020) and microbial activities (Zhu et al., 2022). The customized pore structure in the engineered biochar helps to maintain soil aeration and water-holding capacity (Gong et al., 2019), thereby providing a multifunctional tool for efficient environmental cleanup and sustainable management of As-contaminated agricultural soils (Liu et al., 2022).

Understanding the mechanisms of anionic species interacting with biochars would improve our knowledge of predicting their current and future environmental behavior. Biochar's sorption capacity for anionic nutrients depends on its surface area and functional groups (Table 1). Biochar with a net positive charge has been shown to adsorb more anionic elements than biochar with negative surface charges (Mia et al., 2017a). However, a large negative charge on the biochar surface may attract cations which then attracts anionic nutrients or species, a process known as co-adsorption (Mia et al., 2017a). Thus, the retention of these adsorbed anions through different mechanisms may differ based on the strength of the interactions. Specifically, the direct interactions between biochar surfaces and anionic species (i.e., ionic interactions) can be stronger than those involving co-adsorbed anions (Li et al., 2014; Pan et al., 2021; Wan et al., 2017). Given the diversity of biochar surface properties, the initial properties of biochar have significant implications for predicting their roles in the soil over time. Moreover, the change in biochar properties from positive to negative with aging may also reverse their role in retaining anionic species. Despite biochar adsorption capacities being studied, there is a dearth of information on how surface modification of the same biochars, from positive to negatively charged surfaces, would affect the sorption of anionic species. Hence, the objectives of this study were to develop different functionalized BCs (Mg–Al–Fe, and acid-modified) understand their functionality, and examine how these functionalities are linked to the sorption of negatively charged ions (i.e., phosphate and arsenate).

2. MATERIALS AND METHODS

2.1. Preparation of Biochar

Raw sawdust was collected from a local sawmill and used as the feedstock for preparing biochar. The feedstock was washed with deionized (DI) water to remove dust particles and dried at 80°C overnight. The dry biomass was crushed and sieved to 2 mm before being used for biochar preparation. Biochar was prepared using the slow pyrolysis technique at 500°C for 1 h under a nitrogen flow (Mia et al., 2015). Specifically, the biomass was placed into a crucible and covered using aluminum foil before being pyrolyzed in a muffle furnace. The produced biochar (FBC) was washed and dried at 105°C. The BC was then ground, sieved (<0.12 mm) and stored for further analysis.

Table 1. Effectiveness of doped biochar, activated carbon and biosorbents to reduce arsenic concentration in aqueous solution

Biochar Composite	Main focus	Methods of composite/biochar preparation	Experimental Conditions				Observation	Mechanism	References
			pH	Temperature (°C)	Application rate (g L ⁻¹)	Concentration range (mgL ⁻¹)			
Iron doped amino functionalized sawdust composite	Iron doped amino functionalized sawdust to remove As(III) and As(V) from water.	The synthesis of amino-functionalized sawdust was carried out by modification of raw sawdust with 30% NaOH, followed by reaction with epichlorohydrin and diethylenetriamine at 90 °C, and subsequent washing with acetone, ethanol, and deionized water. Fe (NO ₃) ₃ .9H ₂ O solution was mixed with biomass and oven dried at 90°C for 4h.	7.0 ± 0.2	25	1	1-50	A maximum adsorption of 43.7 mg g ⁻¹ was observed for As (V), whereas, As (III) showed a capacity of 10.1 mg g ⁻¹ .	Iron doped amino-functionalized sawdust composite exhibited a much stronger affinity towards arsenite and arsenate through electrostatic interactions.	Hao et al. (2016)
Iron loaded biochar	Iron loaded biochar to remove As (V) from aqueous solution.	FeCl ₃ .6H ₂ O solution was mixed with biomass and pyrolyzed at 550°C.	7	25	0.1	0.1-5	Adsorption capacity was 1.91 mg g ⁻¹ .	A relatively large surface area (418 m ² /g) contributed to adsorption.	Duan et al. (2017)

Biochar Composite	Main focus	Methods of composite/biochar preparation	Experimental Conditions				Observation	Mechanism	References
			pH	Temperature (°C)	Application rate (g L ⁻¹)	Concentration range (mgL ⁻¹)			
Iron sludge biochar (Fe-SBC) Iron-Mn-La impregnated biochar composite	Fe-SBC was developed from urban sludge for arsenic removal from water.	Pristine biochar was produced from corn stem at 600 °C under N ₂ , then modified by soaking into Fe, Mn, and La solutions followed by pyrolysis at 300 °C to yield Fe-Mn-La-biochar composite with varying La content.	7	25 ± 0.5	1	10-80	An adsorption efficiency of 15.34 mg g ⁻¹ was recorded for As (III)	Adsorption and oxidation were the key mechanisms. As formed La-O-As complex. H ⁺ ions were released during the adsorption process and led to the formation of coordination complexes with La, Fe, and Mn through oxygen bridges.	Lin, Zhang, et al. (2019)
Magnetic biochar (γ-Fe ₂ O ₃)	Agricultural waste was used to produce magnetic biochar enhanced with iron for the adsorption of As (V) from water.	FeCl ₃ .6H ₂ O solution was mixed with biomass and underwent pyrolysis for one hour at 600 °C.	---	22 ± 0.5	2	5-200	The highest capacity of As (V) adsorption was observed at 3.147 mg g ⁻¹ .	Surface complexation was identified as the main adsorption mechanism.	Zhang et al. (2013)
Bismuth impregnated biochar	Preparation of bismuth impregnated BC through wheat straw to remove phosphate and As (III).	A Bi ₂ O ₃ solution was mixed with biomass and subsequently pyrolyzed at 400, 500, and 600 °C for 1 h.	2-10	25	2	The concentration was 60 to 1800 mg L ⁻¹ for phosphate and 5 to 200 mg L ⁻¹ for arsenite.	The maximum adsorption capacities were 125 mg g ⁻¹ for phosphate and 16 mg g ⁻¹ for As (III).	Interactions of phosphate and bismuth were identified as the major mechanism for phosphate, while ligand exchange was the main mechanism for As adsorption.	Zhu et al. (2016)

Biochar Composite	Main focus	Methods of composite/biochar preparation	Experimental Conditions				Observation	Mechanism	References
			pH	Temperature (°C)	Application rate (g L ⁻¹)	Concentration range (mgL ⁻¹)			
Fe and Zr loaded activated carbon	Development of iron and zirconium enhanced activated carbon to identify its potential for As (III) removal from contaminated water.	Biomass waste was pre-treated with FeCl ₃ and the mixture of FeCl ₃ and zirconium oxide (ZrO ₂). Next, the biomass was pyrolyzed at 500 °C for 2 h	7	25	4	0.5	The maximum adsorption capacity of As (III) was 1.206 and 0.679 mg g ⁻¹ for Fe-Zr and Fe-activated carbon, respectively.	Electrostatic attraction and surface complexation were identified as the main mechanisms. Surface functional groups (-OH, -CH ₃ , -CH ₂ , NH ₂ , COO ⁻) specific surface area of the biosorbents considered as a contributor in these processes.	Sahu et al. (2021)
MnO and CuO impregnated biochar composites from Sesbania bispinosa biomass	Potential of Sesbania bispinosa biochar (SBC)-based nanocomposites (for removing As(V) from contaminated wastewater.	A 50 ml CuSO ₄ ·5H ₂ O solution was mixed with 0.25 g biochar produced at 450 °C for 1 h. The mixing was continued for 10 minutes, then titrated with 50 ml of 0.15 M KOH solution. For SBC/MnO, 0.1 M MnCl ₂ solution was used, with the same preparation steps as for SBC/CuO.	4	25±1.5	1	1-10	Maximum As adsorption potential capacities were 12.47 mg g ⁻¹ and 7.35 mg g ⁻¹ for SBC/CuO, and SBC/MnO, respectively	Electrostatic attraction and complexation were identified as the key mechanisms.	Imran et al. (2021)

Biochar Composite	Main focus	Methods of composite/biochar preparation	Experimental Conditions			Observation	Mechanism	References	
			pH	Temperature (°C)	Application rate (g L ⁻¹)				Concentration range (mgL ⁻¹)
Novel α -FeOOH modified wheat straw biochar	An α -FeOOH-modified biochar for simultaneous removal of both Cd(II) and As(III) from the aqueous phase.	α -FeOOH was synthesized via co-precipitation. BC (2.8 g) was activated in 5 mol L ⁻¹ KOH, and then 1 mol L ⁻¹ Fe(NO ₃) ₃ was added to form red precipitates.	4.0 ± 0.1	25	1	54.15	The maximum adsorption capacity of α -FeOOH@BC was 78.3 mg g ⁻¹ which dropped to 67.2 mg g ⁻¹ in Cd and As system.	Co-precipitation and ion exchange were the key mechanisms.	Zhu et al. (2020)
Chemical carbonization of pea peel waste biomass by FeCl ₃ ·6H ₂ O	To investigate the adsorption of arsenic (As) from aqueous solutions using MPAC-500 and MPAC-600 (magnetic-activated carbons synthesized from the peel of <i>Pisum sativum</i> (pea).	Fifteen grams of FeCl ₃ ·6H ₂ O were dissolved in 150 mL deionized water, followed by 30 g of pea peel powder was added. The mixture was pyrolyzed at 500°C (MPAC-500) and 600°C (MPAC-600).	2–10	25–55	0.5–4.0	0.5–2.5	MPAC-500 and MPAC-600 adsorbed As(III) at 0.7297 mg g ⁻¹ and 1.3335 mg g ⁻¹ , respectively, while Q _{max} for As(V) was 0.4930 mg g ⁻¹ and 0.9451 mg g ⁻¹ .	Electrostatic attraction was considered as the key mechanism.	Sahu et al. (2022)

Biochar Composite	Main focus	Methods of composite/biochar preparation	Experimental Conditions			Observation	Mechanism	References	
			pH	Temperature (°C)	Application rate (g L ⁻¹)				Concentration range (mgL ⁻¹)
Novel iron infused biochar developed from Raphanus sativus (MRB) and Artocarpus heterophyllus (MJB).	Evaluation of the adsorption capacity of a modified biochar developed from Radish leaves and Jackfruit peel for removing As(III) and As(V) from aqueous solutions.	An amount of 60 g of powdered feedstock was immersed in FeCl ₃ ·6H ₂ O solution, pre-heated at 80°C for 2 hours, and then pyrolyzed at 800°C in a closed crucible.	3–10	25- 45	1- 3	0.5- 1.5	MRB-800 showed a maximum adsorption capacity (q _{max}) of 2.08 mg g ⁻¹ for As(III) and 2.03 mg g ⁻¹ for As(V), while MJB-800 had q _{max} values of 1.13 mg g ⁻¹ for As(III) and 1.26 mg g ⁻¹ for As(V).	Surface complexation and electrostatic attraction were key mechanisms in As(III and V) adsorption, driven by the functional groups and elemental composition of MRB-800 and MJB-800.	Verma et al. (2022)

The FBC was oxidized by adding 1 g of biochar into 30 mL of 5% H₂O₂ and then heating at 80 °C for 6 h. After evaporation of excess H₂O₂, the oxidized biochar was washed, dried, and adjusted to the pH of fresh biochar. It was then used for characterization and adsorption studies.

The doped biochar (DBC) was produced using a procedure called the doping technique. A total of seven different types of doped BC were produced using different combinations of 0.5 M FeCl₃, MgCl₂·6H₂O, and AlCl₃. Briefly, 5 g of sawdust was mixed with doping chemicals at a ratio of 1:10 (w/v). The prepared mixture was then kept for 12 h to equilibrate with the solutions and then dried at 80°C for another 12 h. The modified biomass was placed into a crucible and sealed with aluminum foil paper. Next, the mineral-loaded biomass was pyrolyzed in a muffle furnace under N₂ flow at 500°C for 1 h. The prepared BCs were then labeled as Mg-doped, Al-doped, Fe-doped, Mg-Al-doped, Mg-Fe-doped, Fe-Al-doped, and Mg-Al-Fe-doped BC, keeping consistency with the added chemicals. All BCs were then washed with DI water to remove non-reacted minerals and dried at 105°C for 4 h. The dried BCs were kept for further chemical analysis and experimentation.

2.2 Cation exchange capacity determination

The cation exchange capacity of biochar was measured by shaking 0.5 g of biochar with 10 mL of 1 M NH₄OAc for 4 h, followed by replacement of NH₄⁺ with Na⁺ using NaOAc (Mia et al., 2017a). Finally, ammonium concentration was determined using the indophenol blue method (Kodama et al., 2015).

2.3 Fourier transform infrared spectroscopy

ATR-FTIR analysis (400–4000 cm⁻¹) was done using 5% biochar in KBr, as per Ascough et al. (2011) and Trompowsky et al. (2005). Peak area under major bands was calculated via Gaussian deconvolution using PeakFit (SAS, Cary, NC). Spectral differences between modified and unmodified biochars were visualized through subtraction.

2.4 Elemental analysis

Total carbon and nitrogen in the biochar were analyzed using an elemental analyzer (FlashSMART, Thermo Fisher Scientific). Ash content is determined by heating samples at 105°C for 4 h to remove moisture (Ismail, 2017), followed by ashing at 730°C for 8–10 h (Aller et al., 2017). Samples were then treated with HNO₃ and H₂O₂, and dried at 120°C. Following cooling, deionized water was added, and samples were vortexed to dissolve the ash residue. Elements such as magnesium (Mg), iron (Fe), and aluminum (Al) concentrations were measured in the extractants using an atomic absorption spectrometer (AA7000- Shimadzu, Japan) (Enders et al., 2012).

2.5 Phosphorus adsorption and desorption study

For the adsorption study, 50 mg L⁻¹ P was used with a background solution of 0.01M CaCl₂. In the batch study, 0.1 g of BC from each sample was added to a 5 mL solution containing 50 ppm in a 50 mL falcon tube. Each treatment was replicated four times. The samples were shaken for 1 h, and

left overnight, then the pH was adjusted to 6.2 using NaOH and HCl. After 7 days of equilibration, the solution was centrifuged and filtered with Whatman No. 42. Next, the solution was analyzed for phosphate using (Murphy & Riley, 1962) method using UV-Vis spectrophotometer (DR6000 UV-VIS Laboratory Spectrophotometer, Hach, Germany)

Adsorbed phosphate at equilibrium (q_e, mg/g) was calculated using Equation 1.

$$q_e = \frac{(C_1 - C_2) * V}{W} \dots\dots\dots [1]$$

Where C₁= Initial concentration of P; C₂= Final concentration of P; V= Volume of solution (L); and W= Mass of biochar (dry basis, g).

After measuring P adsorption capacity, P desorption was measured using the phosphate-loaded-BC samples. Briefly, the residual BC was transferred into falcon tubes, mixed with 5 mL of 0.01 M CaCl₂, and shaken for 2 h at 180 rpm. The mixtures were then filtered, and the extracts analyzed for P concentration as described previously.

2.6 Arsenic adsorption study

A batch experiment was conducted to examine the effect of various BCs on As in soil collected from Kapasia Upazila, Gazipur district (24°04'00.6"N 90°37'04.0"E). The soil is a highly weathered Oxisol with high metal oxides and hydroxides. This study included four treatments, i.e., a) control (collected soil sample), b) soil+ fresh biochar, c) soil+ oxidized biochar, and d) soil+ doped biochar (Mg-Fe-Al doped). To do this, 5 g of air-dried soil (ground and sieved to 2 mm) and 0.1 g of BC from 3 different BC (oxidized, doped and normal BC) samples were mixed thoroughly in a 50 mL falcon tube. Next, 30 mL 100 ppm NaAsO₂ solution was added. The As solution was freshly prepared in DI water. After 7 days of equilibration with intermittent gentle agitation (120 rpm), suspensions were centrifuged and filtered (Whatman No. 42). Arsenic concentration in the filtrates was quantified using a hydride generation atomic absorption spectrophotometer (HGAAS SpectrM 55B, Germany) (Cerveira et al., 2015).

2.7 Statistical Analysis

One-way analysis of variance (ANOVA) was used to examine whether the variation for different treatments was statistically significant while the means were separated following a least-significant difference (LSD) test.

3. RESULTS

3.1 Biochar properties

Biochar production rate varied significantly due to different methods of production (Table 2). The weight of BC was significantly higher when it was produced after loading with minerals than without mineral addition (Table 2). The carbon content was lower in mineral impregnated biochar compared to other BCs. The highest concentration of C (~65.8 %) was found in oxidized biochar which is slightly higher than fresh BC (~64.4%) (Table 2). However, the net cation exchange capacity of fresh BC was larger than Fe-modified BC while it was the highest in the chemically modified biochar.

Table 1. Biochar production rate and mineral content changes with different activation methods (mean \pm SE)

Biochar	Production rate (%)	Concentration of different minerals (%)						CEC (cmol.kg ⁻¹)
		Carbon	Ash content	Fe	Al	Mg	N	
Fresh biochar	29.57 \pm 0.48 c	64.36 \pm 0.0a	3.6 \pm 0.3 c	0.04 \pm 0.0 b	0.04 \pm 0.0 c	1.56 \pm 0.8 b	0.69 \pm 0.0 b	18.2 \pm 2.5 b
Al-doped biochar	61.53 \pm 0.54 a	38.7 \pm 0.5b	17.3 \pm 1.2a	0.04 \pm 0.0 b	3.4 \pm 1.1 a	2.01 \pm 0.4ab	0.53 \pm 0.0 b	2.32 \pm 0.4 c
Fe- doped biochar	64.23 \pm 2.83 a	41 \pm 1.0b	14.8 \pm 1.0ab	1.8 \pm 0.4 a	0.03 \pm 0.0 c	1.52 \pm 0.3 b	0.52 \pm 0.0 b	2.24 \pm 0.2 c
Mg-doped biochar	60.17 \pm 1.34 ab	37 \pm 0.4 b	12.9 \pm 2.4b	0.04 \pm 0.0 b	0.03 \pm 0.0 c	3.50 \pm 1.2 a	0.59 \pm 0.0 b	2.34 \pm 0.4 c
Fe, Al and Mg -doped biochar	53.65 \pm 1.93 b	39 \pm 1.2b	13.8 \pm 0.9ab	1.2 \pm 0.3 ab	0.8 \pm 0.2 b	1.50 \pm 0.7 b	0.53 \pm 0.0 b	2.35 \pm 0.2 c
Chemically oxidized biochar	13.5 \pm 1.4 d	65.8 \pm 0.0 a	2.1 \pm 0.1 c	0.02 \pm 0.0 b	0.02 \pm 0.0 c	0.80 \pm 0.0 c	1.50 \pm 0.0 a	29.3 \pm 1.6 a
P value	<0.01	<0.01	<0.01	<0.01	<0.01	<0.01	<0.01	<0.01

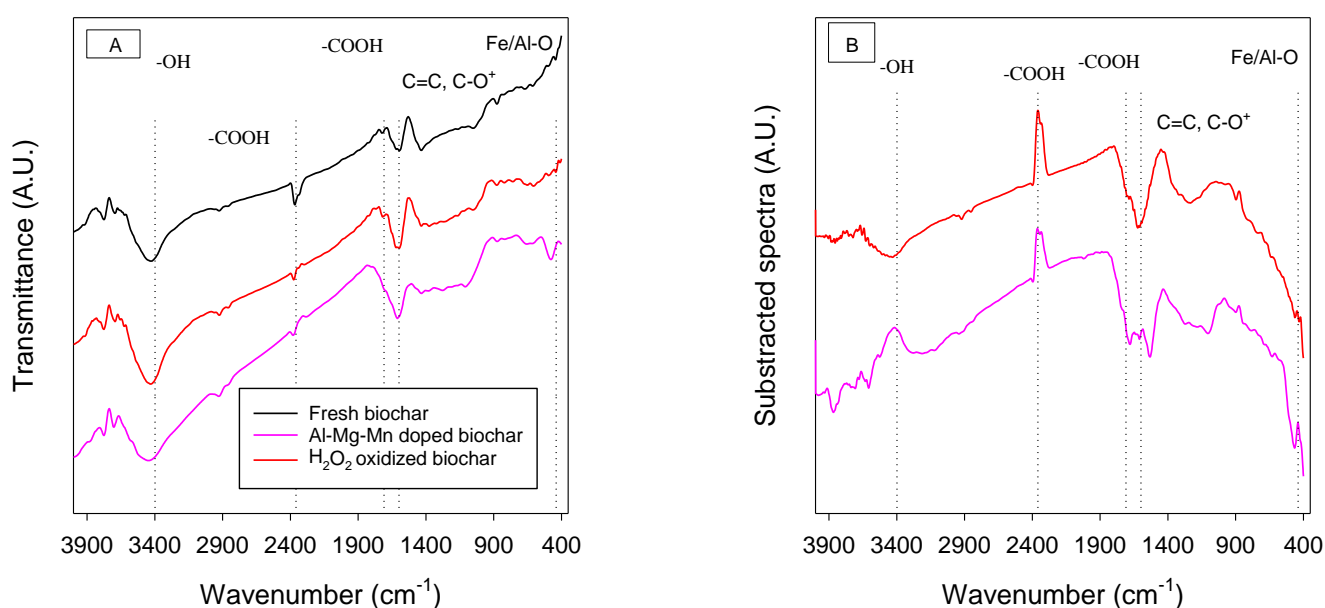


Figure 1. FTIR spectra of fresh, chemically oxidized, and mineral doped biochars. Panel A represents the original spectra while panel B represents the subtracted spectra of chemically oxidized and mineral doped biochar from fresh biochar. Dotted lines indicate different functional groups. Spectra were normalized. For assignment of different functional groups, please see

[Table 3.](#)

3.2 Fourier-transform infrared spectra (FTIR) analysis

Figure 1 illustrates the FTIR spectra of fresh (FBC), oxidized (OBC), and doped (DBC) biochars, emphasizing alterations in surface functional groups. In FBC, peaks at \sim 3400–3800 cm^{-1} , \sim 1720 cm^{-1} , and \sim 1600 cm^{-1} were assigned to hydroxyl stretching, carboxyl, and aromatic C=C vibrations, respectively. The 700–900 cm^{-1} region indicated aromatic C-H out-of-plane bending. For DBC, additional bands at \sim 400 and \sim 700 cm^{-1} reflected Mg–Al–O bonds, while the broad \sim 3450 cm^{-1} peak corresponded to Mg–OH stretching. A minor absorption at \sim 655 cm^{-1} suggested the presence of Fe–O bonds.

3.3 Biochar effects on phosphate adsorption and desorption

Phosphorus adsorption rates were compared across different BCs. Among the BCs, doped-BCs showed significantly higher phosphate adsorption (Fig. 2). The highest

amount of adsorption was demonstrated by Mg-Fe-Al doped-BC, which was about 2.50 mg P g^{-1} BC and followed by Fe-Al, Mg-Fe, Mg-Al, Al, Fe, oxidized and Mg-doped and normal BCs respectively ($P < 0.01$, Fig. 2).

The doped BCs showed significantly greater effectiveness in removing phosphate compared to unmodified BC. Most of the doped BCs adsorbed nearly 100% ($P < 0.01$, Fig. 2). The highest rate was found in Mg-Fe-Al doped-BC.

The desorption study revealed that there was little release of phosphate. However, there was a significant difference in release of adsorbed phosphate among different BCs ($P < 0.01$, Fig. 3A). The Mg-Fe-Al doped BC showed no release of phosphorus after desorption process which demonstrated the best adsorbing capacity. The phosphate desorption was highest in the Fe-DBC which was followed by Mg-DBC, but all the desorption rates were below 0.05 mg/g biochar. In other words, the desorption was below 2.5% of the adsorbed phosphate (Fig. 3B).

Table 2. Peak assignment and relative peak area of different biochars

Functional Group	FBC		OBC		DBC		References
	Peak	Area (%)	Peak	Area (%)	Peak	Area (%)	
Aromatic C-H bending, Mg/Al/Fe-O bonds and Mg-OH stretching	875.68	2.2	605.65	2.3	478.35	1.2	Jung et al. (2017); Pentrák et al. (2018); Wu et al. (2015); Yin et al. (2019); Yang et al. (2022)
					556.0,	0.5	
					580.0, 655.8		
C-O stretching	1051.2	7.5			1109.07	4.4	Arbelaez Breton et al. (2021)
-COOH stretching	1433.11	17.0	1433.11	3.5			Starsinic et al. (1984)
Aromatic C=C, C=O, H-O-H stretching and -OH groups	1597.06	4.0	1595.13	2.9	1610.56	10.6	Arbelaez Breton et al. (2021)
C-H stretching			2860.43	28.2			Singh et al. (2016)
-CH ₂ stretching	2926.01	6.1	2924.09	5.2	2927.94	50.2	Yin et al. (2021)
Mg-OH stretching/	3429.43	57.1	3431.36	53.3	3450.65	33.0	Ahangaran et al. (2013); Kirmizakis et al. (2022)
-OH groups	3774.69	6.1	3776.62	4.6			

Notes: *FBC=fresh biochar; OBC=oxidized biochar; DBC=doped biochar

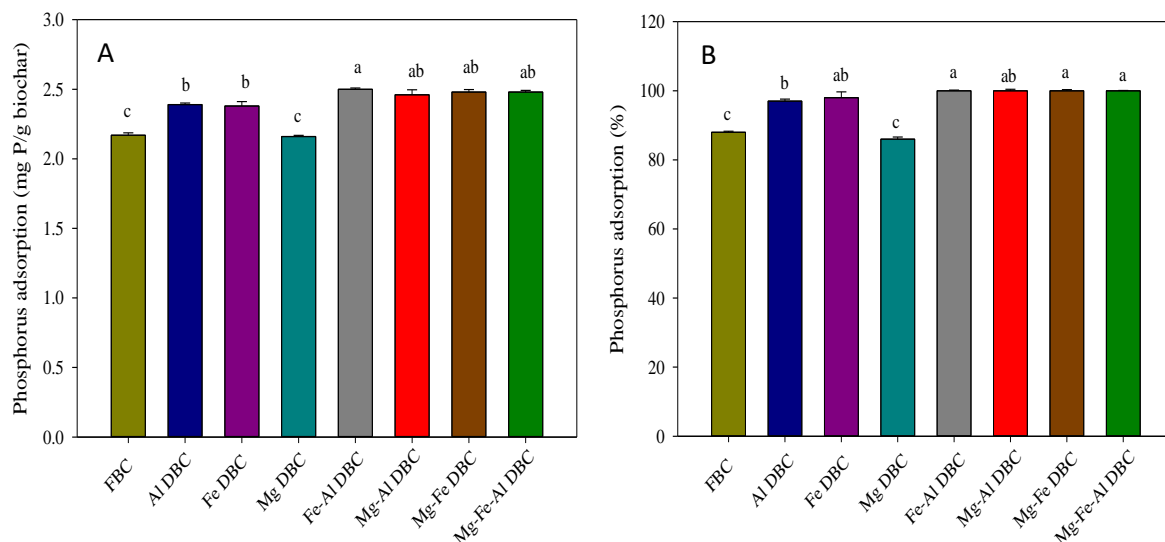


Figure 2. A) Amount of phosphate adsorbed by different Biochar; **B)** Percentages of phosphate adsorption by different biochar. FBC, DBC, and BC represent fresh biochar, doped biochar, and biochar, respectively. Error bar represents the standard error of the mean (N=4).

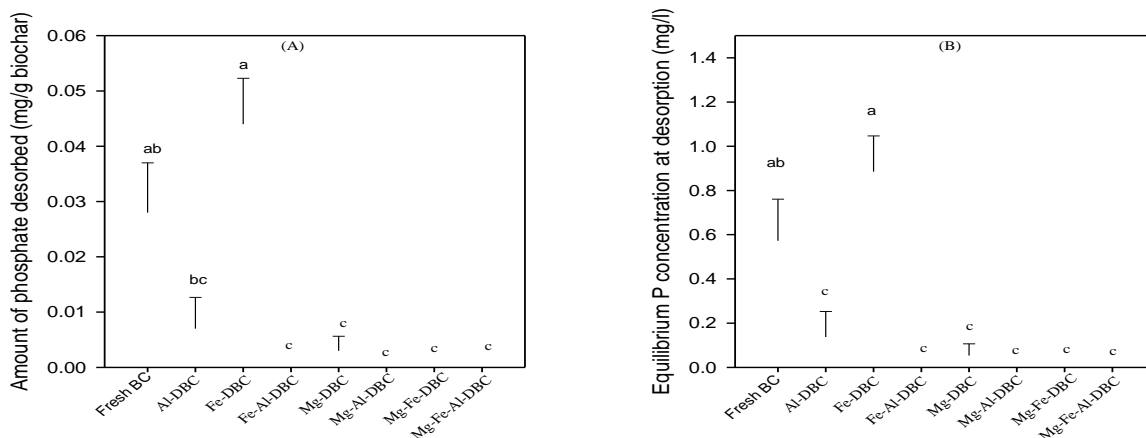


Figure 3. A) Phosphorus desorption by different biochar; **B)** Equilibrium concentration of phosphorus in solution after desorption; FBC, DBC and BC indicate fresh biochar, doped biochar, and biochar, respectively. The error bars represent standard errors of means (N=4).

Table 4. Arsenite (As(III)) adsorption capacity of different modified biochars in comparison to pristine biochars

Control	Treatment/ Activation	As (III) adsorption maxima (Qmax) for pristine biochar (mg g ⁻¹) [#]	As (III) adsorption maxima (Qmax) for modified biochar (mg g ⁻¹)	Change (%)	References
FBC	Post-doped	18.90	31.40	66.1	Samsuri et al. (2013)
FBC	Post-doped	19.30	30.70	59.1	Samsuri et al. (2013)
FBC	Oxidized	0.01	0.01	22.8	Van Vinh et al. (2015)
FBC	Oxidized	2.65	3.97	49.8	Liu et al. (2019)
FBC	Oxidized	2.65	5.67	114.0	Liu et al. (2019)
FBC	Oxidized	2.65	5.14	94.0	Liu et al. (2019)
FBC	Oxidized	2.65	7.03	165.3	Liu et al. (2019)
FBC	Oxidized	2.65	8.74	229.8	Liu et al. (2019)
FBC	Oxidized	2.83	4.02	42.0	Liu et al. (2018)
FBC	Oxidized	2.83	5.16	82.3	Liu et al. (2018)
FBC	Oxidized	2.83	5.26	85.9	Liu et al. (2018)
FBC	Oxidized	2.83	6.40	126.1	Liu et al. (2018)
FBC	Oxidized	2.83	8.47	199.3	Liu et al. (2018)
FBC	Pre-doped	0.00	0.02	731.8	Mondal et al. (2007)
FBC	Oxidized	2.89	4.70	62.6	Lin et al. (2017)
FBC	Oxidized	2.89	8.25	185.5	Lin et al. (2017)
FBC	Oxidized	3.73	14.90	299.5	Lin, Song, et al. (2019)
FBC	Oxidized	2.86	14.77	416.4	Fan et al. (2018)
FBC	Pre-doped	2.67	6.92	159.0	Khan et al. (2020)
FBC	Pre-doped	2.68	7.70	186.8	Khan et al. (2020)
FBC	Post-doped	2.67	17.30	547.1	Khan et al. (2020)
FBC	Post-doped	2.68	28.43	962.1	Khan et al. (2020)
FBC	Pre-doped	0.45	0.52	16.2	Wu et al. (2017)
FBC	Post-doped	1.04	78.30	7428.8	Zhu et al. (2020)

Note: [#]Qmax is the adsorption maxima derived from Langmuir equation fitting to the adsorption isotherms.

Table 5. Arsenite (As(V)) adsorption capacity of different modified biochars in comparison to pristine biochars

Control	Treatment/ Activation	As (V) adsorption maxima (Qmax) for pristine biochar (mg g ⁻¹)	As (V) adsorption maxima (Qmax) for modified biochar (mg g ⁻¹)	Change (%)	References
FBC	Post-doped	5.50	15.20	176.4	Samsuri et al. (2013)
FBC	Post-doped	7.1	16.90	138.0	Samsuri et al. (2013)
FBC	Pre-doped	0.27	0.43	61.7	Wang, Gao, Zimmerman, et al. (2015)
FBC	Oxidized	0.79	108.88	13682.3	Liang et al. (2020)
FBC	Pre-doped	10.30	28.49	176.6	Nguyen et al. (2019)
FBC	Pre-doped	0.55	5.90	968.8	Wu et al. (2017)
FBC	Post-doped	24.49	30.98	26.5	Jin et al. (2014)
FBC	Pre-doped	4.26	4.32	1.4	Hussain et al. (2020)
FBC	Pre-doped	4.26	4.48	5.2	Hussain et al. (2020)
FBC	Oxidized	5.08	39.44	676.1	Frišták et al. (2018)
FBC	Oxidized	5.08	34.90	586.8	Frišták et al. (2018)
FBC	Post-doped	256.00	457.00	78.5	Alchouron et al. (2020)
FBC	Post-doped	217.00	868.00	300.0	Alchouron et al. (2020)
FBC	Post-doped	.002	0.01	431.3	Wongrod et al. (2018)
FBC	Post-doped	17.50	45.80	161.7	Zhou et al. (2017)
FBC	Pre-doped	0.20	0.59	195.0	Wang, Gao, Li, et al. (2015)
FBC	Oxidized	0.20	0.91	355.0	Wang, Gao, Li, et al. (2015)

3.4 Biochar effect on arsenite adsorption

The concentration of As in soil was affected significantly due to different BC additions ($P < 0.01$, Fig. 4, Table 4, and 5). The highest As adsorption was with doped BC which was followed by then oxidized BC. The initial concentration of As

in soil was about 0.6 mg As/g soil which was then reduced to 0.1 mg As/g soil with the addition of doped BC. But no significant changes were observed with the addition of normal BC compared to control (without biochar) treatment (Fig. 4).

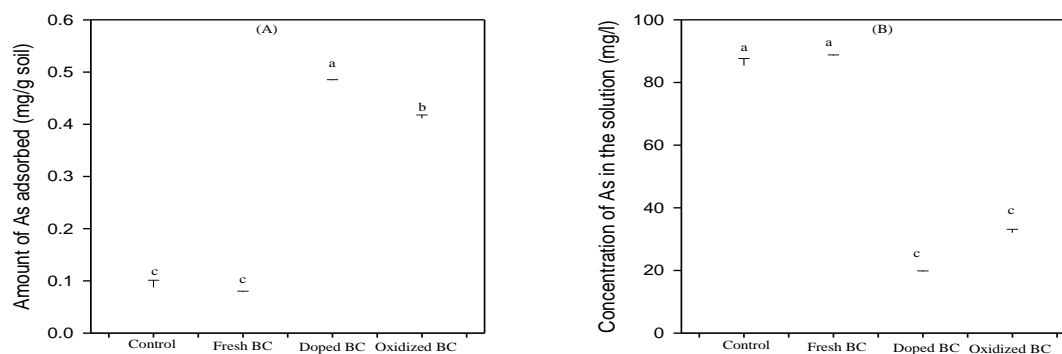


Figure 4. A) Amount of arsenic adsorption onto different biochars amended oxisol; B) Equilibrium arsenic concentration in different treatments after adsorption. Error bar represents standard errors.

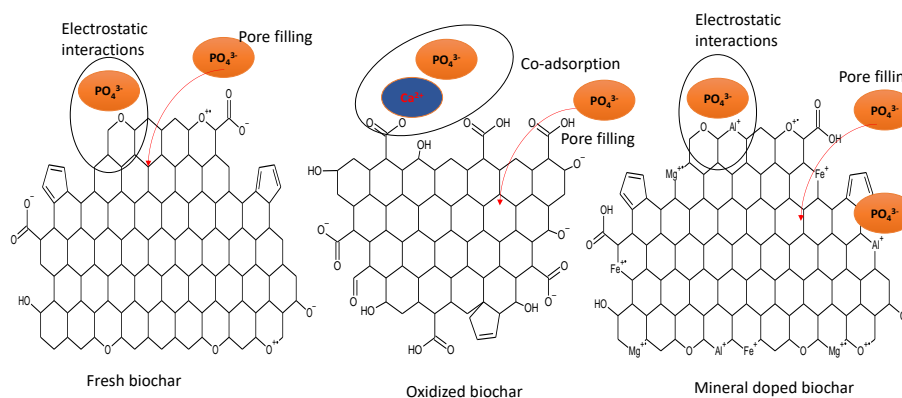


Figure 5. Mechanism of phosphate adsorption to different biochar surfaces.

4. DISCUSSION

Biochar's large specific surface area and surface functional groups enable it to adsorb various ionic nutrients, including phosphate (Mia et al., 2017a). However, the relative adsorption capacity of biochar depends on the net surface charge of biochar. Positive surfaces can be created with the impregnation of minerals (e.g. Fe, Al, and Mg), and thus, the adsorption capacity can be increased (Peng et al., 2021; Zhang et al., 2020). In our study, we in fact observed a significant increase in the adsorption of phosphate with mineral-impregnated biochar. Our elemental and FTIR analysis clearly showed that minerals were impregnated into the biochar (Table 2 and Fig. 1). Specifically, doped biochar showed Mg-Al-O vibrations at ~ 400 and 700 cm^{-1} , with Mg-OH stretching at 478 cm^{-1} and 3450 cm^{-1} (Akgül et al., 2019; Hou et al., 2023; Micháleková-Richveisová et al., 2017; Peng et al., 2021; Saadat et al., 2018). FTIR bands at $\sim 655\text{ cm}^{-1}$ confirmed the presence of Fe-O (Jung et al., 2017; Penetrák et al., 2018; Wu et al., 2015; Yang et al., 2022).

The relative adsorption capacity of different mineral-doped BCs was similar, but relatively higher when Fe, Al and Mg were used in combination. Similar to our study, it has also been reported that phosphate adsorption increased with doping. The adsorption of phosphate with mineral-doped BC may mostly be due to the ionic interactions of phosphate with the positive surfaces of BCs (Fig. 5). Since the impregnation of mineral creates positive surfaces on the BC (Shakoor et al., 2020; Zhu et al., 2019) and these positive surfaces might have attracted negatively charged phosphate. Moreover, pore

filling (i.e., physical adsorption) might also have contributed partially (Akgül et al., 2018; Hou et al., 2023; Micháleková-Richveisová et al., 2017; Peng et al., 2021; Saadat et al., 2018). However, the contribution of weak binding mechanisms such as physical adsorption might be negligible since the rate of desorption of the adsorbed phosphate is low (<5%).

Doped and oxidized biochar significantly ($P < 0.01$) reduced soil As levels (Fig. 4). Doped biochar decreased As by 77%, and oxidized biochar by 63%, compared to the control. Fresh biochar showed no significant effect on As concentration in soil solution, indicating limited impact on As bioavailability. Soil with Fe and Al oxides and hydroxides can fix negatively charged ions, including arsenite (Suda & Makino, 2016). However, this binding can be disrupted by competing organic compounds such as humic and fulvic acids. The application of positively charged BC can increase positive surfaces in soil and thus, increase adsorption anionic species including arsenite (Fig. 6, Akgül et al. (2018); Hou et al. (2023); Micháleková-Richveisová et al. (2017); Peng et al. (2021); Saadat et al. (2018)), In this study, arsenic adsorption increased notably with doped biochars. Synthesis of literature data showed similar results (Table 4 & 5), showing that chemically modified biochars both pre and post-doped- exhibited greater As retention than fresh BC. This is likely due to increased surface area, enriched positive functional groups, and synergistic effects of mineral doping through co-adsorption (Fig. 6). In the case of oxidized BC, the improved As adsorption may result mainly from increased surface area and some co-adsorption with cations (Fig.6).

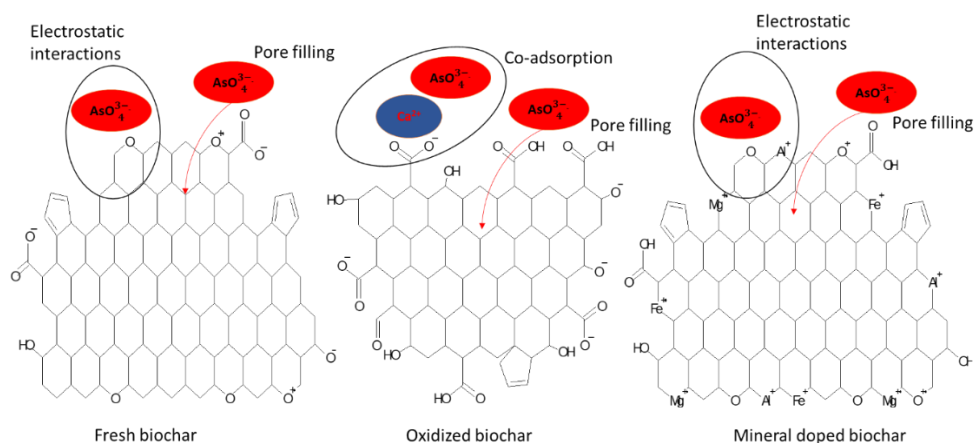


Figure 6. Mechanism of arsenic adsorption to different biochar surfaces.

These suggest that functionalization could enhance biochar's utility in environmental remediation and nutrient management. Still, long-term studies are needed to understand the stability of adsorbed contaminants and the mechanisms involved under dynamic soil conditions.

5. CONCLUSION

The present study was to investigate the efficacy of different BCs in reducing As contamination in soil. A batch adsorption study conducted against phosphate was conducted in the laboratory to identify the effectiveness of normal BC, oxidized BC, and Mg-Fe-Al DBC/LDH-doped biochar. The results show that oxidized and doped BC has the potential to reduce the As concentration in soil by 63% and 77% respectively. However, there was no significant effect of non-modified BC in reducing As toxicity in plants.

Declaration of Competing Interest

The authors declare that no competing financial or personal interests may appear to influence the work reported in this paper.

References

- Abney, R. B., & Berhe, A. A. (2018). Pyrogenic Carbon Erosion: Implications for Stock and Persistence of Pyrogenic Carbon in Soil [Review]. *Frontiers in Earth Science, Volume 6* - 2018. <https://doi.org/10.3389/feart.2018.00026>
- Ahangaran, F., Hassanzadeh, A., & Nouri, S. (2013). Surface modification of Fe₃O₄@SiO₂ microsphere by silane coupling agent. *International Nano Letters, 3*(1), 23. <https://doi.org/10.1186/2228-5326-3-23>
- Akgül, G., Maden, T. B., Diaz, E., & Jiménez, E. M. (2018). Modification of tea biochar with Mg, Fe, Mn and Al salts for efficient sorption of PO₄³⁻ and Cd²⁺ from aqueous solutions. *Journal of Water Reuse and Desalination, 9*(1), 57-66. <https://doi.org/10.2166/wrd.2018.018>
- Alchouron, J., Navarathna, C., Chludil, H. D., Dewage, N. B., Perez, F., Hassan, E. B., . . . Mlsna, T. E. (2020). Assessing South American Guadua chacoensis bamboo biochar and Fe₃O₄ nanoparticle dispersed analogues for aqueous arsenic(V) remediation. *Science of The Total Environment, 706*, 135943. <https://doi.org/10.1016/j.scitotenv.2019.135943>
- Aller, D., Bakshi, S., & Laird, D. A. (2017). Modified method for proximate analysis of biochars. *Journal of Analytical and Applied Pyrolysis, 124*, 335-342. <https://doi.org/10.1016/j.jaap.2017.01.012>
- Arbelaez Breton, L., Mahdi, Z., Pratt, C., & El Hanandeh, A. (2021). Modification of Hardwood Derived Biochar to Improve Phosphorus Adsorption. *Environments, 8*(5), 41. <https://doi.org/10.3390/environments8050041>
- Arslan, B., Djamgoz, M. B. A., & Akün, E. (2017). ARSENIC: A Review on Exposure Pathways, Accumulation, Mobility and Transmission into the Human Food Chain. In P. de Voogt & F. A. Gunther (Eds.), *Reviews of Environmental Contamination and Toxicology Volume 243* (pp. 27-51). Springer International Publishing. https://doi.org/10.1007/398_2016_18
- Ascough, P. L., Bird, M. I., Francis, S. M., & Lebl, T. (2011). Alkali extraction of archaeological and geological charcoal: evidence for diagenetic degradation and formation of humic acids. *Journal of Archaeological Science, 38*(1), 69-78. <https://doi.org/10.1016/j.jas.2010.08.011>
- Beesley, L., Marmiroli, M., Pagano, L., Pignoni, V., Fellet, G., Fresno, T., . . . Marmiroli, N. (2013). Biochar addition to an arsenic contaminated soil increases arsenic concentrations in the pore water but reduces uptake to tomato plants (*Solanum lycopersicum* L.). *Science of The Total Environment, 454-455*, 598-603. <https://doi.org/10.1016/j.scitotenv.2013.02.047>
- Caporale, A. G., & Violante, A. (2016). Chemical Processes Affecting the Mobility of Heavy Metals and Metalloids in Soil Environments. *Current Pollution Reports, 2*(1), 15-27. <https://doi.org/10.1007/s40726-015-0024-y>
- Cerveira, C., Pozebon, D., de Moraes, D. P., & Silva de Fraga, J. C. (2015). Speciation of inorganic arsenic in rice using hydride generation atomic absorption spectrometry (HG-AAS) [10.1039/C5AY00563A]. *Analytical Methods, 7*(11), 4528-4534. <https://doi.org/10.1039/C5AY00563A>

- Cotrufo, M. F., Boot, C., Abiven, S., Foster, E. J., Haddix, M., Reisser, M., . . . Schmidt, M. W. I. (2016). Quantification of pyrogenic carbon in the environment: An integration of analytical approaches. *Organic Geochemistry*, 100, 42-50. <https://doi.org/10.1016/j.orggeochem.2016.07.007>
- Duan, X., Zhang, C., Srinivasakannan, C., & Wang, X. (2017). Waste walnut shell valorization to iron loaded biochar and its application to arsenic removal. *Resource-Efficient Technologies*, 3(1), 29-36. <https://doi.org/10.1016/j.reffit.2017.01.001>
- Enders, A., Hanley, K., Whitman, T., Joseph, S., & Lehmann, J. (2012). Characterization of biochars to evaluate recalcitrance and agronomic performance. *Bioresource Technology*, 114, 644-653. <https://doi.org/10.1016/j.biortech.2012.03.022>
- Fan, J., Xu, X., Ni, Q., Lin, Q., Fang, J., Chen, Q., . . . Lou, L. (2018). Enhanced As (V) Removal from Aqueous Solution by Biochar Prepared from Iron-Impregnated Corn Straw. *Journal of Chemistry*, 2018(1), 5137694. <https://doi.org/10.1155/2018/5137694>
- Frišták, V., Moreno-Jiménez, E., Fresno, T., & Diaz, E. (2018). Effect of Physical and Chemical Activation on Arsenic Sorption Separation by Grape Seeds-Derived Biochar. *Separations*, 5(4), 59. <https://doi.org/10.3390/separations5040059>
- Ghezzi, L., Arrighi, S., Petrini, R., Bini, M., Vittori Antisari, L., Franceschini, F., . . . Giannecchini, R. (2023). Arsenic Contamination in Groundwater, Soil and the Food-Chain: Risk Management in a Densely Populated Area (Versilia Plain, Italy). *Applied Sciences*, 13(9), 5446. <https://doi.org/10.3390/app13095446>
- Gong, H., Tan, Z., Zhang, L., & Huang, Q. (2019). Preparation of biochar with high absorbability and its nutrient adsorption-desorption behaviour. *Science of The Total Environment*, 694, 133728. <https://doi.org/10.1016/j.scitotenv.2019.133728>
- Hao, L., Zheng, T., Jiang, J., Zhang, G., & Wang, P. (2016). Removal of As(III) and As(V) from water using iron doped amino functionalized sawdust: Characterization, adsorptive performance and UF membrane separation. *Chemical Engineering Journal*, 292, 163-173. <https://doi.org/10.1016/j.cej.2016.01.097>
- Hou, C., Xiu, W., Guo, H., Li, S., & Jiang, C. (2023). Application of Al-Fe Co-modified Rice-Straw Biochar to Fluoride Removal: Synthesis, Optimization, and Performance. *Water, Air, & Soil Pollution*, 234(3), 169. <https://doi.org/10.1007/s11270-023-06172-4>
- Hussain, M., Imran, M., Abbas, G., Shahid, M., Iqbal, M., Naeem, M. A., . . . Ul Islam, A. (2020). A new biochar from cotton stalks for As (V) removal from aqueous solutions: its improvement with H₃PO₄ and KOH. *Environmental Geochemistry and Health*, 42(8), 2519-2534. <https://doi.org/10.1007/s10653-019-00431-2>
- Imran, M., Iqbal, M. M., Iqbal, J., Shah, N. S., Khan, Z. U. H., Murtaza, B., . . . Rizwan, M. (2021). Synthesis, characterization and application of novel MnO and CuO impregnated biochar composites to sequester arsenic (As) from water: Modeling, thermodynamics and reusability. *Journal of Hazardous Materials*, 401, 123338. <https://doi.org/10.1016/j.jhazmat.2020.123338>
- Ismail, B. P. (2017). Ash Content Determination. In *Food Analysis Laboratory Manual* (pp. 117-119). Springer International Publishing. https://doi.org/10.1007/978-3-319-44127-6_11
- Jin, H., Capareda, S., Chang, Z., Gao, J., Xu, Y., & Zhang, J. (2014). Biochar pyrolytically produced from municipal solid wastes for aqueous As(V) removal: Adsorption property and its improvement with KOH activation. *Bioresource Technology*, 169, 622-629. <https://doi.org/10.1016/j.biortech.2014.06.103>
- Jung, K.-W., Jeong, T.-U., Choi, J.-W., Ahn, K.-H., & Lee, S.-H. (2017). Adsorption of phosphate from aqueous solution using electrochemically modified biochar calcium-alginate beads: Batch and fixed-bed column performance. *Bioresource Technology*, 244, 23-32. <https://doi.org/10.1016/j.biortech.2017.07.133>
- Khan, Z. H., Gao, M., Qiu, W., & Song, Z. (2020). Efficient As(III) Removal by Novel MoS₂-Impregnated Fe-Oxide-Biochar Composites: Characterization and Mechanisms. *ACS Omega*, 5(22), 13224-13235. <https://doi.org/10.1021/acsomega.0c01268>
- Kirmizakis, P., Tawabini, B., Siddiq, O. M., Kalderis, D., Ntarlagiannis, D., & Soupios, P. (2022). Adsorption of Arsenic on Fe-Modified Biochar and Monitoring Using Spectral Induced Polarization. *Water*, 14(4), 563. <https://doi.org/10.3390/w14040563>
- Kodama, T., Ichikawa, T., Hidaka, K., & Furuya, K. (2015). A highly sensitive and large concentration range colorimetric continuous flow analysis for ammonium concentration. *Journal of Oceanography*, 71(1), 65-75. <https://doi.org/10.1007/s10872-014-0260-6>
- Li, Y., Shao, J., Wang, X., Deng, Y., Yang, H., & Chen, H. (2014). Characterization of Modified Biochars Derived from Bamboo Pyrolysis and Their Utilization for Target Component (Furfural) Adsorption. *Energy & Fuels*, 28(8), 5119-5127. <https://doi.org/10.1021/ef500725c>
- Liang, M., Lu, L., He, H., Li, J., Zhu, Z., & Zhu, Y. (2021). Applications of Biochar and Modified Biochar in Heavy Metal Contaminated Soil: A Descriptive Review. *Sustainability*, 13(24), 14041. <https://doi.org/10.3390/su132414041>
- Liang, T., Li, L., Zhu, C., Liu, X., Li, H., Su, Q., . . . Li, F. (2020). Adsorption of As(V) by the Novel and Efficient Adsorbent Cerium-Manganese Modified Biochar. *Water*, 12(10), 2720. <https://doi.org/10.3390/w12102720>
- Lin, L., Qiu, W., Wang, D., Huang, Q., Song, Z., & Chau, H. W. (2017). Arsenic removal in aqueous solution by a novel Fe-Mn modified biochar composite: Characterization and mechanism. *Ecotoxicology and Environmental Safety*, 144, 514-521. <https://doi.org/10.1016/j.ecoenv.2017.06.063>
- Lin, L., Song, Z., Khan, Z. H., Liu, X., & Qiu, W. (2019). Enhanced As(III) removal from aqueous solution by Fe-Mn-La-impregnated biochar composites. *Science of The Total Environment*, 694, 133728. <https://doi.org/10.1016/j.scitotenv.2019.133728>

- Environment*, 686, 1185-1193. <https://doi.org/10.1016/j.scitotenv.2019.05.480>
- Lin, L., Zhang, G., Liu, X., Khan, Z. H., Qiu, W., & Song, Z. (2019). Synthesis and adsorption of FeMnLa-impregnated biochar composite as an adsorbent for As(III) removal from aqueous solutions. *Environmental Pollution*, 247, 128-135. <https://doi.org/10.1016/j.envpol.2019.01.044>
- Liu, X., Gao, M., Qiu, W., Khan, Z. H., Liu, N., Lin, L., & Song, Z. (2019). Fe–Mn–Ce oxide-modified biochar composites as efficient adsorbents for removing As(III) from water: adsorption performance and mechanisms. *Environmental Science and Pollution Research*, 26(17), 17373-17382. <https://doi.org/10.1007/s11356-019-04914-8>
- Liu, X., Zhang, G., Lin, L., Khan, Z. H., Qiu, W., & Song, Z. (2018). Synthesis and Characterization of Novel Fe–Mn–Ce Ternary Oxide–Biochar Composites as Highly Efficient Adsorbents for As(III) Removal from Aqueous Solutions. *Materials*, 11(12), 2445. <https://doi.org/10.3390/ma11122445>
- Liu, Z., Xu, Z., Xu, L., Buyong, F., Chay, T. C., Li, Z., . . . Wang, X. (2022). Modified biochar: synthesis and mechanism for removal of environmental heavy metals. *Carbon Research*, 1(1), 8. <https://doi.org/10.1007/s44246-022-00007-3>
- Mia, S., Dijkstra, F. A., & Singh, B. (2017a). Aging Induced Changes in Biochar's Functionality and Adsorption Behavior for Phosphate and Ammonium. *Environmental Science & Technology*, 51(15), 8359-8367. <https://doi.org/10.1021/acs.est.7b00647>
- Mia, S., Dijkstra, F. A., & Singh, B. (2017b). Chapter One - Long-Term Aging of Biochar: A Molecular Understanding With Agricultural and Environmental Implications. In D. L. Sparks (Ed.), *Advances in Agronomy* (Vol. 141, pp. 1-51). Academic Press. <https://doi.org/10.1016/bs.agron.2016.10.001>
- Mia, S., Uddin, N., Mamun Hossain, S. A. A., Amin, R., Mete, F. Z., & Hiemstra, T. (2015). Production of Biochar for Soil Application: A Comparative Study of Three Kiln Models. *Pedosphere*, 25(5), 696-702. [https://doi.org/10.1016/S1002-0160\(15\)30050-3](https://doi.org/10.1016/S1002-0160(15)30050-3)
- Micháleková-Richveisová, B., Frišták, V., Pipiška, M., Ďuriška, L., Moreno-Jimenez, E., & Soja, G. (2017). Iron-impregnated biochars as effective phosphate sorption materials. *Environmental Science and Pollution Research*, 24(1), 463-475. <https://doi.org/10.1007/s11356-016-7820-9>
- Mondal, P., Balo Majumder, C., & Mohanty, B. (2007). Removal of Trivalent Arsenic (As(III)) from Contaminated Water by Calcium Chloride (CaCl₂)-Impregnated Rice Husk Carbon. *Industrial & Engineering Chemistry Research*, 46(8), 2550-2557. <https://doi.org/10.1021/ie060702i>
- Murphy, J., & Riley, J. P. (1962). A modified single solution method for the determination of phosphate in natural waters. *Analytica Chimica Acta*, 27, 31-36. [https://doi.org/10.1016/S0003-2670\(00\)88444-5](https://doi.org/10.1016/S0003-2670(00)88444-5)
- Namgay, T., Singh, B., & Singh, B. P. (2010). Influence of biochar application to soil on the availability of As, Cd, Cu, Pb, and Zn to maize (*Zea mays* L.). *Soil Research*, 48(7), 638-647. <https://doi.org/10.1071/SR10049>
- Nguyen, T. H., Pham, T. H., Nguyen Thi, H. T., Nguyen, T. N., Nguyen, M.-V., Tran Dinh, T., . . . Thi, V. H. T. (2019). Synthesis of Iron-Modified Biochar Derived from Rice Straw and Its Application to Arsenic Removal. *Journal of Chemistry*, 2019(1), 5295610. <https://doi.org/10.1155/2019/5295610>
- Pan, S.-Y., Dong, C.-D., Su, J.-F., Wang, P.-Y., Chen, C.-W., Chang, J.-S., . . . Hung, C.-M. (2021). The Role of Biochar in Regulating the Carbon, Phosphorus, and Nitrogen Cycles Exemplified by Soil Systems. *Sustainability*, 13(10), 5612. <https://doi.org/10.3390/su13105612>
- Peng, Y., Sun, Y., Fan, B., Zhang, S., Bolan, N. S., Chen, Q., & Tsang, D. C. W. (2021). Fe/Al (hydr)oxides engineered biochar for reducing phosphorus leaching from a fertile calcareous soil. *Journal of Cleaner Production*, 279, 123877. <https://doi.org/10.1016/j.jclepro.2020.123877>
- Pentrák, M., Hronský, V., Pálková, H., Uhlík, P., Komadel, P., & Madejová, J. (2018). Alteration of fine fraction of bentonite from Kopernica (Slovakia) under acid treatment: A combined XRD, FTIR, MAS NMR and AES study. *Applied Clay Science*, 163, 204-213. <https://doi.org/10.1016/j.clay.2018.07.028>
- Reisser, M., Purves, R. S., Schmidt, M. W. I., & Abiven, S. (2016). Pyrogenic Carbon in Soils: A Literature-Based Inventory and a Global Estimation of Its Content in Soil Organic Carbon and Stocks [Original Research]. *Frontiers in Earth Science*, Volume 4 - 2016. <https://doi.org/10.3389/feart.2016.00080>
- Saadat, S., Raei, E., & Talebbeydokhti, N. (2018). Enhanced removal of phosphate from aqueous solutions using a modified sludge derived biochar: Comparative study of various modifying cations and RSM based optimization of pyrolysis parameters. *Journal of Environmental Management*, 225, 75-83. <https://doi.org/10.1016/j.jenvman.2018.07.037>
- Sahu, N., Nayak, A. K., Verma, L., Bhan, C., Singh, J., Chaudhary, P., & Yadav, B. C. (2022). Adsorption of As(III) and As(V) from aqueous solution by magnetic biosorbents derived from chemical carbonization of pea peel waste biomass: Isotherm, kinetic, thermodynamic and breakthrough curve modeling studies. *Journal of Environmental Management*, 312, 114948. <https://doi.org/10.1016/j.jenvman.2022.114948>
- Sahu, N., Singh, J., & Koduru, J. R. (2021). Removal of arsenic from aqueous solution by novel iron and iron–zirconium modified activated carbon derived from chemical carbonization of *Tectona grandis* sawdust: Isotherm, kinetic, thermodynamic and breakthrough curve modelling. *Environmental Research*, 200, 111431. <https://doi.org/10.1016/j.envres.2021.111431>
- Samsuri, A. W., Sadegh-Zadeh, F., & Seh-Bardan, B. J. (2013). Adsorption of As(III) and As(V) by Fe coated biochars

- and biochars produced from empty fruit bunch and rice husk. *Journal of Environmental Chemical Engineering*, 1(4), 981-988. <https://doi.org/10.1016/j.jece.2013.08.009>
- Shakoor, M. B., Shafaqat, A., Muhammad, R., Farhat, A., Irshad, B., Muhammad, R., . . . and Rinklebe, J. (2020). A review of biochar-based sorbents for separation of heavy metals from water. *International Journal of Phytoremediation*, 22(2), 111-126. <https://doi.org/10.1080/15226514.2019.1647405>
- Singh, B., Fang, Y., & Johnston, C. T. (2016). A Fourier-Transform Infrared Study of Biochar Aging in Soils. *Soil Science Society of America Journal*, 80(3), 613-622. <https://doi.org/10.2136/sssaj2015.11.0414>
- Singh, P., Rawat, S., Jain, N., Bhatnagar, A., Bhattacharya, P., & Maiti, A. (2023). A review on biochar composites for soil remediation applications: Comprehensive solution to contemporary challenges. *Journal of Environmental Chemical Engineering*, 11(5), 110635. <https://doi.org/10.1016/j.jece.2023.110635>
- Starsinic, M., Otake, Y., Walker, P. L., & Painter, P. C. (1984). Application of FT-i.r. spectroscopy to the determination of COOH groups in coal. *Fuel*, 63(7), 1002-1007. [https://doi.org/10.1016/0016-2361\(84\)90325-9](https://doi.org/10.1016/0016-2361(84)90325-9)
- Strawn, D. G. (2018). Review of interactions between phosphorus and arsenic in soils from four case studies. *Geochemical Transactions*, 19(1), 10. <https://doi.org/10.1186/s12932-018-0055-6>
- Suda, A., & Makino, T. (2016). Functional effects of manganese and iron oxides on the dynamics of trace elements in soils with a special focus on arsenic and cadmium: A review. *Geoderma*, 270, 68-75. <https://doi.org/10.1016/j.geoderma.2015.12.017>
- Trompowsky, P. M., Benites, V. d. M., Madari, B. E., Pimenta, A. S., Hockaday, W. C., & Hatcher, P. G. (2005). Characterization of humic like substances obtained by chemical oxidation of eucalyptus charcoal. *Organic Geochemistry*, 36(11), 1480-1489. <https://doi.org/10.1016/j.orggeochem.2005.08.001>
- Ungureanu, G., Santos, S., Boaventura, R., & Botelho, C. (2015). Arsenic and antimony in water and wastewater: Overview of removal techniques with special reference to latest advances in adsorption. *Journal of Environmental Management*, 151, 326-342. <https://doi.org/10.1016/j.jenvman.2014.12.051>
- Van Vinh, N., Zafar, M., Behera, S. K., & Park, H. S. (2015). Arsenic(III) removal from aqueous solution by raw and zinc-loaded pine cone biochar: equilibrium, kinetics, and thermodynamics studies. *International Journal of Environmental Science and Technology*, 12(4), 1283-1294. <https://doi.org/10.1007/s13762-014-0507-1>
- Verma, L., Akanksha, A., & Singh, J. (2022). Performance of a novel iron infused biochar developed from *Raphanus sativus* and *Artocarpus heterophyllus* refuse for trivalent and pentavalent arsenic adsorption from an aqueous solution: mechanism, isotherm and kinetics study. *International Journal of Phytoremediation*, 24(9), 919-932. <https://doi.org/10.1080/15226514.2021.1985078>
- Wan, S., Wang, S., Li, Y., & Gao, B. (2017). Functionalizing biochar with Mg–Al and Mg–Fe layered double hydroxides for removal of phosphate from aqueous solutions. *Journal of Industrial and Engineering Chemistry*, 47, 246-253. <https://doi.org/10.1016/j.jiec.2016.11.039>
- Wang, L., O'Connor, D., Rinklebe, J., Ok, Y. S., Tsang, D. C. W., Shen, Z., & Hou, D. (2020). Biochar Aging: Mechanisms, Physicochemical Changes, Assessment, And Implications for Field Applications. *Environmental Science & Technology*, 54(23), 14797-14814. <https://doi.org/10.1021/acs.est.0c04033>
- Wang, S., Gao, B., Li, Y., Mosa, A., Zimmerman, A. R., Ma, L. Q., . . . Migliaccio, K. W. (2015). Manganese oxide-modified biochars: Preparation, characterization, and sorption of arsenate and lead. *Bioresource Technology*, 181, 13-17. <https://doi.org/10.1016/j.biortech.2015.01.044>
- Wang, S., Gao, B., Zimmerman, A. R., Li, Y., Ma, L., Harris, W. G., & Migliaccio, K. W. (2015). Removal of arsenic by magnetic biochar prepared from pinewood and natural hematite. *Bioresource Technology*, 175, 391-395. <https://doi.org/10.1016/j.biortech.2014.10.104>
- Wongrod, S., Simon, S., van Hullebusch, E. D., Lens, P. N. L., & Guibaud, G. (2018). Changes of sewage sludge digestate-derived biochar properties after chemical treatments and influence on As(III and V) and Cd(II) sorption. *International Biodeterioration & Biodegradation*, 135, 96-102. <https://doi.org/10.1016/j.ibiod.2018.10.001>
- Wu, C., Huang, L., Xue, S.-G., Huang, Y.-Y., Hartley, W., Cui, M.-q., & Wong, M.-H. (2017). Arsenic sorption by red mud-modified biochar produced from rice straw. *Environmental Science and Pollution Research*, 24(22), 18168-18178. <https://doi.org/10.1007/s11356-017-9466-7>
- Wu, M., Feng, Q., Sun, X., Wang, H., Gielen, G., & Wu, W. (2015). Rice (*Oryza sativa* L) plantation affects the stability of biochar in paddy soil. *Scientific Reports*, 5(1), 10001. <https://doi.org/10.1038/srep10001>
- Yan, X., Yang, W., Chen, X., Wang, M., Wang, W., Ye, D., & Wu, L. (2020). Soil Phosphorus Pools, Bioavailability and Environmental Risk in Response to the Phosphorus Supply in the Red Soil of Southern China. *International Journal of Environmental Research and Public Health*, 17(20), 7384. <https://doi.org/10.3390/ijerph17207384>
- Yang, Y., Piao, Y., Wang, R., Su, Y., Liu, N., & Lei, Y. (2022). Nonmetal function groups of biochar for pollutants removal: A review. *Journal of Hazardous Materials Advances*, 8, 100171. <https://doi.org/10.1016/j.hazadv.2022.100171>
- Yin, D., Wang, X., Peng, B., Tan, C., & Ma, L. Q. (2017). Effect of biochar and Fe-biochar on Cd and As mobility and transfer in soil-rice system. *Chemosphere*, 186, 928-937. <https://doi.org/10.1016/j.chemosphere.2017.07.126>

- Yin, G., Tao, L., Chen, X., Bolan, N. S., Sarkar, B., Lin, Q., & Wang, H. (2021). Quantitative analysis on the mechanism of Cd²⁺ removal by MgCl₂-modified biochar in aqueous solutions. *Journal of Hazardous Materials*, 420, 126487. <https://doi.org/10.1016/j.jhazmat.2021.126487>
- Yin, W., Zhao, C., Xu, J., Zhang, J., Guo, Z., & Shao, Y. (2019). Removal of Cd(II) and Ni(II) from aqueous solutions using activated carbon developed from powder-hydrolyzed-feathers and *Trapa natans* husks. *Colloids and Surfaces A: Physicochemical and Engineering Aspects*, 560, 426-433. <https://doi.org/10.1016/j.colsurfa.2018.10.031>
- Zhang, J., Hou, D., Shen, Z., Jin, F., O'Connor, D., Pan, S., . . . Alessi, D. S. (2020). Effects of excessive impregnation, magnesium content, and pyrolysis temperature on MgO-coated watermelon rind biochar and its lead removal capacity. *Environmental Research*, 183, 109152. <https://doi.org/10.1016/j.envres.2020.109152>
- Zhang, M., Gao, B., Varnoosfaderani, S., Hebard, A., Yao, Y., & Inyang, M. (2013). Preparation and characterization of a novel magnetic biochar for arsenic removal. *Bioresource Technology*, 130, 457-462. <https://doi.org/10.1016/j.biortech.2012.11.132>
- Zhou, Z., Liu, Y.-g., Liu, S.-b., Liu, H.-y., Zeng, G.-m., Tan, X.-f., . . . Cai, X.-x. (2017). Sorption performance and mechanisms of arsenic(V) removal by magnetic gelatin-modified biochar. *Chemical Engineering Journal*, 314, 223-231. <https://doi.org/10.1016/j.cej.2016.12.113>
- Zhu, D., Ma, J., Li, G., Rillig, M. C., & Zhu, Y.-G. (2022). Soil plastispheres as hotspots of antibiotic resistance genes and potential pathogens. *The ISME Journal*, 16(2), 521-532. <https://doi.org/10.1038/s41396-021-01103-9>
- Zhu, N., Qiao, J., & Yan, T. (2019). Arsenic immobilization through regulated ferrollysis in paddy field amendment with bismuth impregnated biochar. *Science of The Total Environment*, 648, 993-1001. <https://doi.org/10.1016/j.scitotenv.2018.08.200>
- Zhu, N., Yan, T., Qiao, J., & Cao, H. (2016). Adsorption of arsenic, phosphorus and chromium by bismuth impregnated biochar: Adsorption mechanism and depleted adsorbent utilization. *Chemosphere*, 164, 32-40. <https://doi.org/10.1016/j.chemosphere.2016.08.036>
- Zhu, S., Qu, T., Irshad, M. K., & Shang, J. (2020). Simultaneous removal of Cd(II) and As(III) from co-contaminated aqueous solution by α-FeOOH modified biochar. *Biochar*, 2(1), 81-92. <https://doi.org/10.1007/s42773-020-00040-8>